

**SPLICED CONNECTIONS FOR ADJACENT PRECAST MEMBER BRIDGES USING
ULTRA AND VERY HIGH PERFORMANCE CONCRETE**

Kedar R. Halbe, Via Dept. of Civil Engineering, Virginia Tech, Blacksburg, VA

Carrie Field, Via Dept. of Civil Engineering, Virginia Tech, Blacksburg, VA

Patrick Joyce, Via Dept. of Civil Engineering, Virginia Tech, Blacksburg, VA

Carin Roberts-Wollmann, PhD, PE, Via Dept. of Civil Engineering, Virginia Tech,
Blacksburg, VA

Thomas Cousins, PhD, PE, Via Dept. of Civil Engineering, Virginia Tech, Blacksburg, VA

ABSTRACT

Spliced connections in the longitudinal joints of bridges with adjacent precast members are investigated as an alternative to the current grouted shear key connection. The minimum splice lengths are determined for No. 4 and No. 6 bars using fiber reinforced ultra and very high performance concretes (UHPC and VHPC) as connection materials. The minimum splice length is determined experimentally using simply supported reinforced concrete beam specimens with tension splices formed within a pocket filled with the fiber reinforced connection material. The test results are verified using a strain compatibility analysis of the beam specimens to confirm the yielding of tension steel. The experimental and analytical results show that the minimum splice length with No. 4 bars is 4 in. and that with No. 6 bars is 6 in. The conclusions made in this research show that UHPC and VHPC can be used to reduce the length of tension splices and these connections can be applied in longitudinal joints of adjacent precast member bridges.

Keywords: Adjacent Precast Members, Connections, Ultra High Performance Concrete, Tension Splices, Experimental Testing, and Strain Compatibility.

INTRODUCTION

Bridges with adjacent precast members (APM) are a suitable system for short spans, locations with low clearances and for accelerated bridge construction or replacement. This bridge system offers inherent advantages of economy, rapid construction and high torsional stiffness. However, the occurrence of reflective cracks in the deck persists to be the “Achilles heel” for this quick to implement and economical bridge system. The issue of reflective cracks in composite or non-composite toppings of bridges with adjacent precast box beam bridges has been prevalent since the very first details for the bridge system were devised and implemented. Through research, experimentation and experience the connection details have been updated to explore solutions to prevent or at least abate reflective cracking in bridges with adjacent precast members. Presented in this research is an alternative method sought to alleviate the issue of shear key failure and reflective cracking by establishing a spliced connection between adjacent box beam and voided slab bridges. This paper is focused on the experimental and analytical work performed to establish the minimum length of splice required to form a connection of sufficient strength and ductility.

ADJACENT PRECAST MEMBER BRIDGE CONNECTIONS

The issues of shear key failure and associated reflective cracks in the bridge topping have been extensively detailed in the state-of-the-art report by Russell (2009). Traditionally, the APM bridge beam connections have made the use of a grouted shear key detail, partial or full beam depth and transverse post-tensioning (PT) to produce a monolithic behavior in the bridge superstructure. It has been observed in the US that the traditional detail has been susceptible to failure. Moreover, the transverse PT has proven to be insufficient in producing a uniform monolithic behavior in the superstructure. Transverse PT is most effective at the discrete locations of application. The compressive effect of transverse PT is reduced progressively at locations further from point of application. As shear key failure is initiated in the joints of the APM bridge system, the load distribution between adjacent beams is adversely affected. Essentially, the traditional grouted connection has proven to be insufficient in resisting the shears and especially the moments generated on the connection by traffic loads, intrinsic loads such as shrinkage and environmental effects such as temperature gradients.

In this research an alternative means to achieve connections between adjacent beams is sought. The main focus of this research is to incorporate a structural connection between adjacent members that can resist the aforementioned load effects. To that means, a spliced connection between adjacent members is proposed. This paper outlines the concepts of the testing program focused on establishing the minimum length of splice required to provide sufficient strength and ductility to the connection. The results of the experimental program and the analysis performed to verify the results are discussed.

SPECIMEN DETAILS

The specimens were comprised of an 8.5 ft long simply supported reinforced concrete beam with a pocket and disconnected reinforcing bars in the midspan to form the splice connection.

For purpose of discussion the specimens are described by three components: the precast element, the splice pocket and the interface between the precast element and the pocket. The cross-sectional size of the pocket was kept consistent between specimens. The length of the pocket was varied according to the splice length under consideration. The main tension reinforcement was either two No. 4 bars or No. 6 bars depending on the specimen. The area of compression steel was varied between the beam specimens. Initial specimens had equal areas of steel in tension and compression. The area of steel in compression was increased after the initial tests. The reasons for increase in compression area are explained with the test results.

The beam specimens were designed such that the failure would occur within the region of the splice. The beam design was carried out as follows,

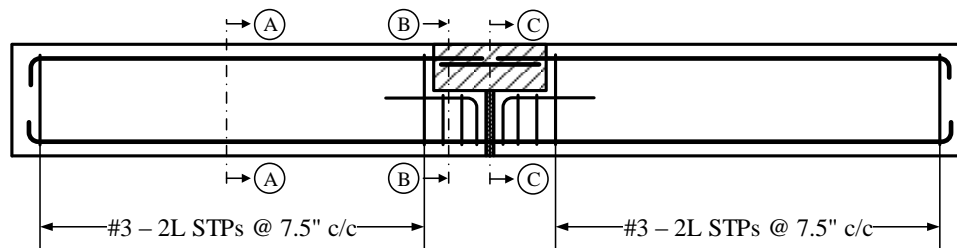


Figure 1. Typical details of beam specimens.

1. The capacity of the beam at Section C-C of Figure 1 was calculated by assuming typical properties of UHPC/VHPC and reinforcing steel.
2. The moment capacity was then assumed to be the bending moment subjected Section C-C of the beam and the externally applied loads were calculated.
3. Bending moments at Sections A-A and B-B were calculated and were compared with the beam capacities at the respective sections. Both sections had sufficient capacity to resist the bending moments.
4. Shear reinforcement was designed to prevent shear failure in the beam.

The splice pockets were filled with either a proprietary UHPC available commercially or the very high performance concrete (VHPC), with a mix design developed by the researchers. VHPC is not a typically used term and was used by the researchers since the material properties of this mix were below what constitutes the UHPC designation. Typical UHPC is defined as “cementitious based composite materials with discontinuous fiber reinforcement, compressive strengths above 21.7 ksi pre-and post-cracking tensile strengths above 0.72 ksi and enhanced durability via their discontinuous pore structure” by Russell and Graybeal (2013).

Table 1 presents the mix designs for the two filler materials. The proportions presented in Table 1 are from Graybeal (2006) and represent a typical formulation for UHPC. The VHPC

mix design was developed using proportions presented in Morcous et al. (Spring 2011) as a starting point, but adding 1 in. long steel fibers to provide tensile strength.

Table 1. UHPC and VHPC Mixture Proportions.

Constituent	UHPC (lb/cu. ft.)	VHPC (lb/cu. ft.)
Cement	44.44	41.50
Silica Fume	14.44	8.90
Fly Ash	NA	8.90
Ground Quartz	13.15	NA
Fine Sand	63.7	53.70
¼ in Max Coarse Aggregate	NA	23.00
Water	6.82	11.80
Superplasticizer	1.92	0.75 – 1.05
Steel fibers	9.74	9.80
Water/Cementitious	0.12	0.20

The typical details of the test specimens are summarized in Table 2 and the typical details are shown in Figure 2. The specimen nomenclature is as follows:

U/V-BR-SL-NO-DS

Where,

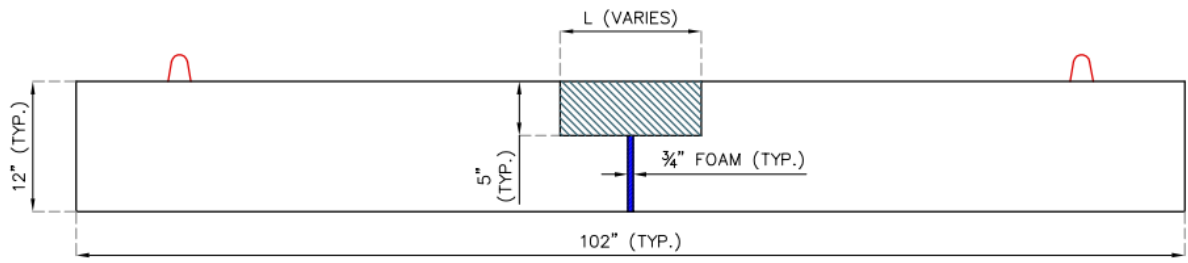
U/V = Material used in pocket. U = UHPC, V = VHPC.

BR = Tension reinforcing bar size (No.4 or No. 6).

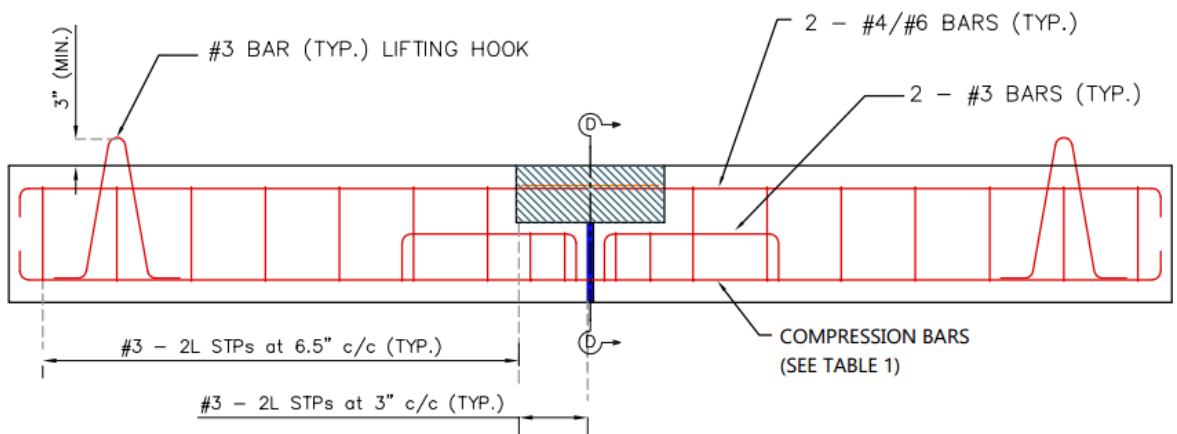
SL = Length of splice (in.).

NO = Serial number for each specimen type on the basis of splice lengths.

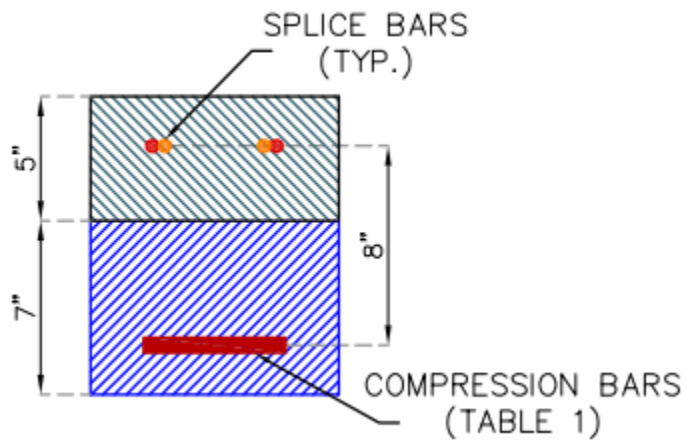
DS = Specimen design. E = equal area of steel in tension and compression.



(a) Elevation of splice test specimens.



(b) Sectional elevation and reinforcement details.



(c) Detail D-D

Figure 2. Typical details of beam specimens.

Table 2. Test Matrix.

Specimen Designation	Tension Steel	Splice Length (in.)	Pocket Length (in.)	Pocket Filler	Compression Steel	Concrete Strength (ksi.)
U-4-5-I-E	2 No. 4s	5	11	UHPC	2 No. 4s	8
U-4-6-I-E		6	13		2 No. 7s and 1 No. 6	5
U-4-3-I		3	7			
U-4-4-I		4	9			
U-4-5-II		5	11			
V-4-5-I		VHPC	5	11	2 No. 8s	5
V-4-6-I			6	13	2 No. 8s	5
V-4-5-II			5	15	2 No. 8s	5
V-4-3-I			3	17	2 No. 8s	5
V-4-4-I			4	21	2 No. 8s	5
V-4-4-II			4	9	2 No. 8s	5
U-6-5-I-E			2 No. 6s	5	11	UHPC
U-6-6-I-E	6	13		2 No. 8s and 1 No. 7	5	
U-6-7-I	7	15				
U-6-8-I	8	17				

A critical piece of information needed from the testing was the stress in the spliced reinforcing bars. To determine if a splice length is adequate to develop the yield strength of the bar, the stress in the bar must be known. Unfortunately, this measurement cannot be made directly with a bonded electrical resistance strain gauge on the tension steel, because the waterproofing required to protect the gauge from the concrete destroys the bond between the bar and the concrete. Instead, the compression bars were instrumented with strain gauges. A $\frac{3}{4}$ in. thick foam pad was placed in the formwork at the beam midspan such that the compressive force at that section would be carried by the reinforcement only. This was expected to simplify the calculation of the stress in the tension reinforcement by eliminating the uncertainty in determining the moment arm between the tension and compression forces in the beam. The free body diagram of specimen section at the area of interest is shown in Figure 3. However, the calculation of the neutral axis depth and consequently the lever arm could not be avoided, this will be discussed in the results section of the paper.

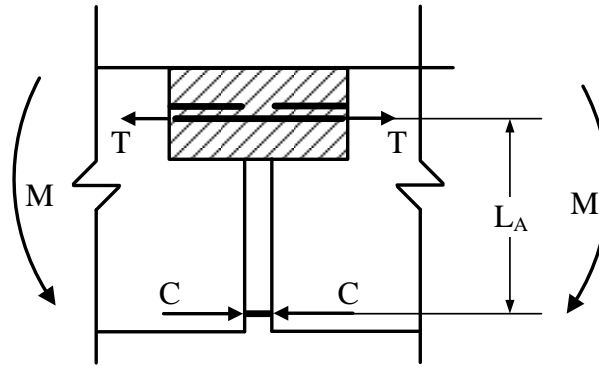


Figure 3. Free body diagram of the specimen at the area of interest.

TEST SETUP

The test setup, shown in Figure 4, consisted of a simply supported beam tested in an upside down configuration. The test configuration placed the splice in the region of maximum constant bending moment. The specimens were tested in an inverted configuration so that the cracking patterns in the UHPC pocket could easily be observed. The load applied through the actuator was measured by a single load cell (maximum capacity 50 kips). Vertical deflections were measured by three wire potentiometers connected to the beam ends and midspan of the beam. The interface between UHPC and beam concrete was instrumented with LVDTs (on the east face) to observe the occurrence of cracks at the concrete – UHPC interface. The reinforcement in the compression zone was instrumented with strain gauges. Additionally, locating discs for a DEMEC (DEmountable MEchanical) extensometer were attached to the top of the UHPC pocket and the west face of all specimens to measure surface deformations at different depths at midspan (top fiber, tensile reinforcement depth, mid-depth of beam and compressive reinforcement depth).

PROCEDURE

The specimens were typically tested seven to nine days after the placement of the pocket forming material. Both materials, UHPC and VHPC, have a rapid strength gain and provide the potential of early age application such as accelerated bridge construction. The loads from a single actuator were distributed equally and applied at the beam ends through a spreader beam. The supports were placed at a distance of 3 in. from the beam end. The clear span between the face of the loading frame and the closest support was 27 in. This clear span was sufficient to prevent the beam ends from acting as a deep beam, which is twice the depth of the beam as per ACI 318.

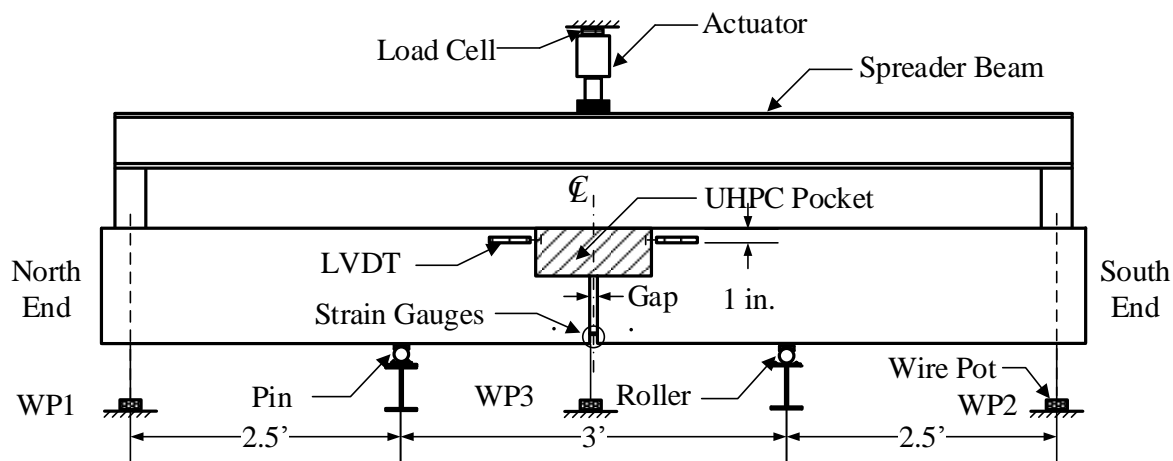


Figure 4. Test Setup.

The loading on the beams was applied at pre-determined increments with pauses to mark cracks and make DEMEC measurements. Load increments of 1000 – 2000 lb were applied to specimens with No. 4 bars until the first crack in the UHPC pocket was observed. The load application was then increased to 2500 – 3000 lb. Similarly, load increments of 2000 – 3000 lb were applied to specimens with No. 6 bars followed by increments of 5000 – 6000 lb after the first crack in the pocket was observed. The data acquisition system was programmed to read and record data at 10 Hz. Although the test itself was static, it was important to record the response of the specimen to instantly changing conditions such as the occurrence of cracks or tension reinforcement slip. The data recording was started after the specimen was positioned on the supports prior to the placement of the spreader beam. Hence, the test data does not directly include the effect of self-weight of the specimen on the test results. The effect of self-weight was found to be small in comparison to applied loads on the results of the splice tests.

MATERIALS USED IN TESTING AND PROPERTIES

The material properties of the precast element concrete, steel reinforcement and the pocket filler materials were measured as per relevant ASTM guidelines as shown in Table 3

Table 3. Material testing guidelines.

Test	Specimen	Material	Standard
Compressive Strength	4 in. × 8in. Cylinders	Conventional Concrete and VHPC	ASTM C39 / AASHTO T22
Compressive Strength	2 in. × 2 in. Cubes	UHPC	ASTM C109 / AASHTO T106
Splitting Tensile Strength	4 in. × 8in. Cylinders	Conventional Concrete, UHPC and VHPC	ASTM C496 / AASHTO T198
Modulus of Elasticity	4 in. × 8in. Cylinders		ASTM C469

Typically, the modulus of elasticity and compressive and splitting tensile strengths of the pocket filler material were measured on the day of the test. As mentioned before, the material properties of UHPC and VHPC were tested seven to nine days after mixing. The precast element compressive strength was also measured on the day of the test while the material properties of the steel reinforcement were tested after the conclusion of beam tests. The typical material properties are summarized in Table 4.

Table 4. Typical material properties of materials used in testing.

Specimens	Precast Concrete Compressive Strength (psi)	Filler Material		Steel Reinforcement Yield Stress (ksi)			
		Compressive Strength (psi)	Tensile Strength (psi)*	No. 4	No. 6	No. 7	No. 8
UHPC with equal area of reinforcement	7360	13200 - 23800	2200 - 3000	62	60	NA	NA
UHPC with unequal area of reinforcement	3900	13200 - 23800	2200 - 3000	62	60	62	69.5
VHPC	4700 - 4900	12400 - 13800	1600 - 1800	69	NA	NA	69.5

NOTE: * denotes split cylinder tensile strength.

TEST RESULTS

This section presents test observations and measurements. Refer to Table 2 for specimen designation. The test results are presented separately for specimens with No. 4 bars and specimens with No. 6 bars.

SPLICES WITH NO. 4 BARS AND UHPC AND VHPC SPLICE POCKET FILLER

The splice lengths tested with No. 4 bars range from 3 in. to 6 in. The UHPC tests were performed in two stages. Specimens U-4-5-I-E and U-4-6-I-E were the first beams tested. The area of steel in tension and compression was equal that is, two No. 4 bars were used. Specimens U-4-3-I and U-4-4-I and U-4-5-II were tested in the second phase of testing. The area of steel in compression was increased to provide resistance to the added tensile strength provided by the pocket filler material until the separation of the interface between the pocket and the precast element. The specimens with UHPC as pocket filler material were tested first. After observing the results from the UHPC tests, the VHPC specimens were designed with two No. 4 bars as tension reinforcement and two No. 8 bars as compression reinforcement.

The nominal strengths of the specimens were calculated based on the yield strength of the tension reinforcement and the moment arm between the compression and tension

reinforcement. For this basic calculation, the contribution of the UHPC to flexural strength is ignored.

$$A_s = 0.2 \text{ in}^2 \times 2 = 0.4 \text{ in}^2$$

$$M_n = A_s f_y \times \text{moment arm} = 0.4 \text{ in}^2 \times 60 \text{ ksi} \times 8 \text{ in.} = 192 \text{ in-k}$$

Based on the loading diagram presented in Figure 4, the applied load to result in a 192 in-k moment is:

$$M = \frac{P_{\text{applied}}}{2} \times 30 \text{ in.}$$

$$P_{\text{applied}} = \frac{M}{15 \text{ in.}} = \frac{192 \text{ in-k}}{15 \text{ in.}} = 12.8 \text{ kips}$$

The failure load calculated thus was compared with the peak loads applied to each specimen to ensure that tension steel yielding had indeed occurred in the specimen. The load vs. deflection behavior of the specimens with No.4 bars is shown in Figure 5 and Figure 6. Figure 5 shows the average of the deflections at the two beam ends, while Figure 6 shows the deflection at midspan. The load vs. deflection plots show that the peak loads for all specimens were larger than the calculated design load. This does not necessarily indicate that all specimens had sufficient splice length. This could result if the pocket filler material was providing tensile capacity such that the applied loads were higher than the calculated ultimate load. This possibility was further ratified by observing the load vs. interface displacement shown in Figure 7. The x-axis values in Figure 7 pertain to the LVDT that recorded the maximum value of displacement at either interface. It can be observed that the plot appears to be linear until about a total load of 15000 lb is applied. Above this load the interface separates and produces the conditions assumed for the calculation of ultimate load.

Another important observation made in these tests was that the deflection values in the beam midspan did not increase significantly until the occurrence of interface separation. A similar behavior is observed in the plot of load vs. compressive strain as shown in Figure 8. The values of compressive strain plotted in Figure 8 are the average values of the two strain gauges. The occurrence of non-linear behavior corresponds with the separation of the interface with the exception of specimens U-4-5-I-E and U-4-6-I-E. In those specimens the compression steel yielded at much lower loads since the compressive region had a much smaller capacity than the tensile region of the beam. This was the primary reason that the area of steel was increased for the remainder of the tests. The prevention of compression steel yielding was desired for the ease of calculation of strains and stresses in the tension reinforcement. The added area of steel did not seem to work as designed since the non-linear behavior indicates that the compression reinforcement did actually yield. The compression bar yielding is further explained in the analysis and discussion section of the paper. Typically, a longer splice length produced a more ductile behavior as expected. Moreover, the VHPC specimens displayed the most ductile behavior. The test results of specimens with No. 4 bars are summarized in Table 5.

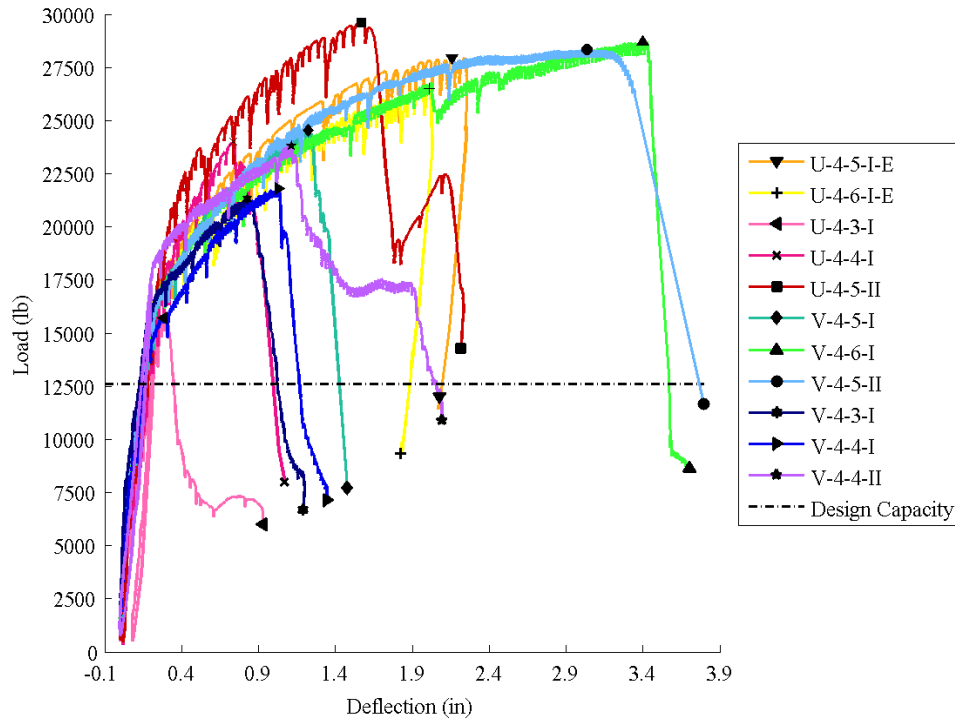


Figure 5. Load vs. average end deflection for specimens with No. 4 bars.

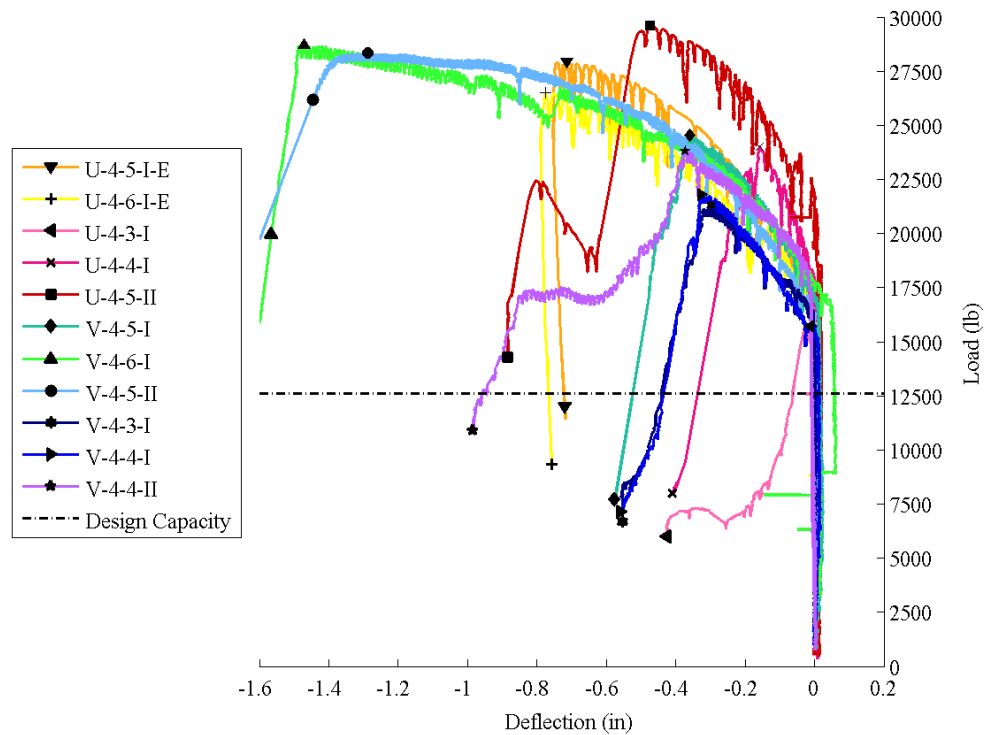


Figure 6. Load vs. midspan deflection for specimens with No. 4 bars (note that upward displacement is negative).

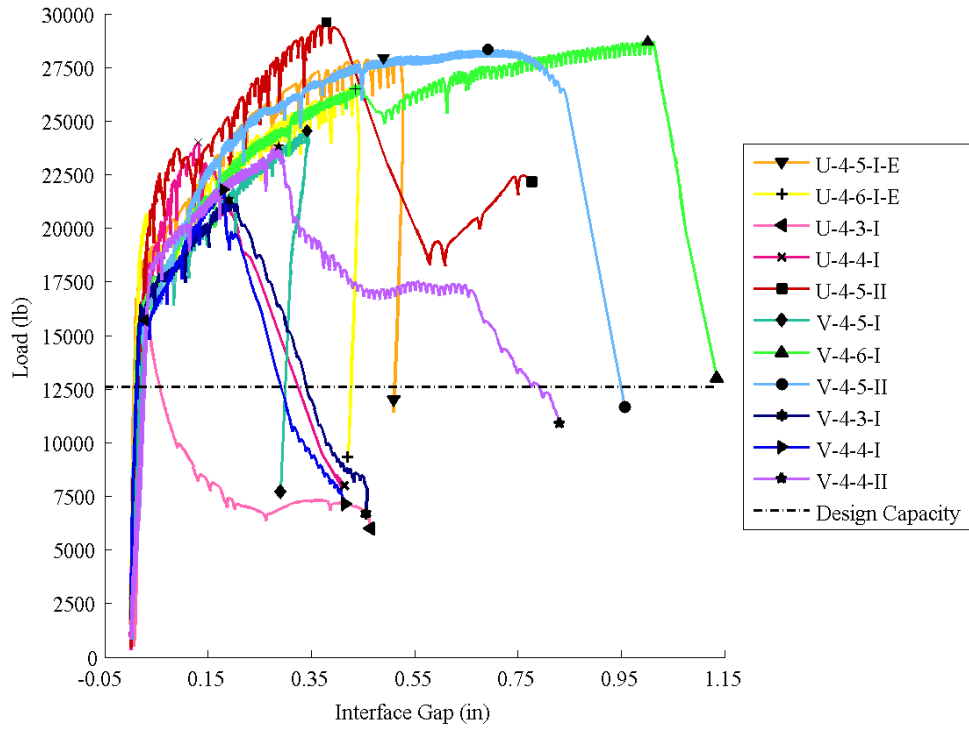


Figure 7. Load vs. interface displacement for specimens with No. 4 bars.

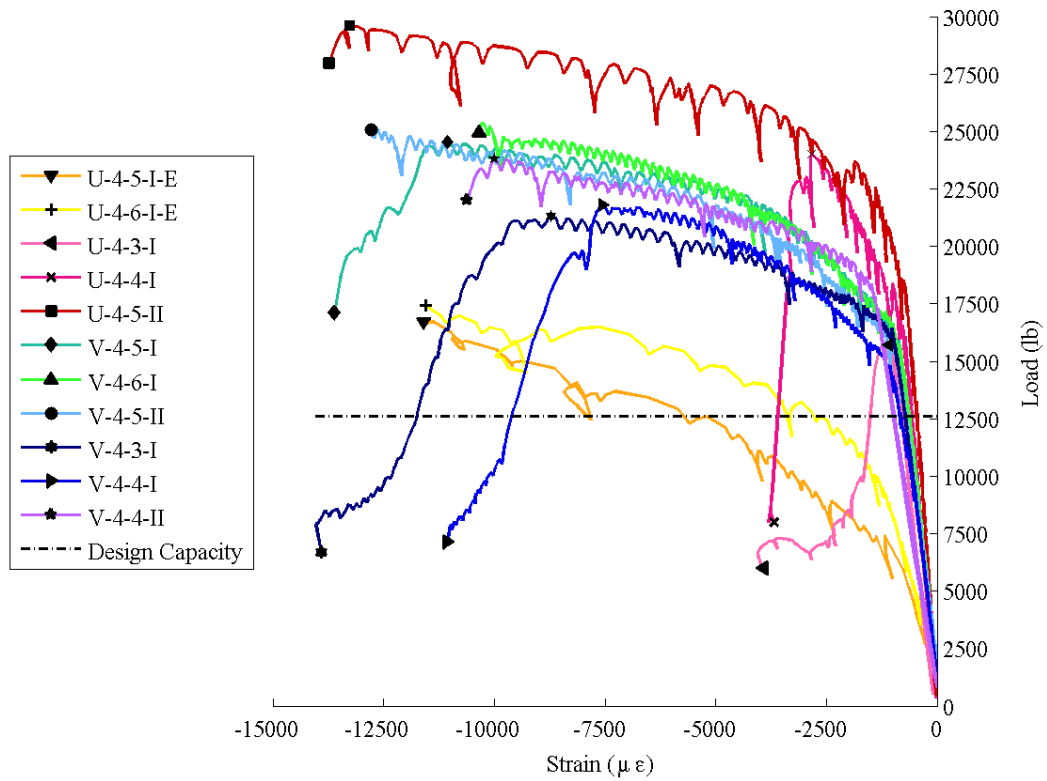


Figure 8. Load vs. average reinforcement bar strain for specimens with No.4 bars.

Table 5. Test Results for Specimens with No. 4 Bars

Specimen Designation	Splice Length, in.	Compression Reinforcement	First Cracking Load, lbs	Maximum Load, lbs	Failure Modes
U-4-5-I-E	5	2 No. 4s	7200	27,900	NA
U-4-6-I-E	6	2 No. 4s	6900	26,500	NA
U-4-3-I	3	2 No.7s and 1 No. 6	5800	15,700	Rebar slip
U-4-4-I	4	2 No.7s and 1 No. 6	7500	24,600	Splitting
U-4-5-II	5	2 No.7s and 1 No. 6	9000	29,600	Splitting
V-4-5-I	5	2 No. 8s	3,200	24,600	Splitting
V-4-6-I	6	2 No. 8s	3,000	28,700	Splitting
V-4-5-II	5	2 No. 8s	1,500	28,300	Rupture
V-4-3-I	3	2 No. 8s	1,000	21,300	Splitting
V-4-4-I	4	2 No. 8s	2,000	21,800	Rebar slip
V-4-4-II	4	2 No. 8s	1,500	23,800	Splitting

It is apparent in comparing the load corresponding to the nominal capacity to the failure loads presented in Table 5 that all specimens exceeded the yield moment, indicating all tension reinforcement had yielded at the instant of failure. For the UHPC specimens, repeating the same calculations with the ultimate strength of the No. 4 reinforcing bars, of 102 ksi indicates that the bars would be expected to rupture at an applied load of 21.8 kips. Interestingly, four of five specimens exceeded this capacity, and none failed due to bar rupture. However, other aspects of the specimens' behavior must be investigated to determine an appropriate splice length. For the VHPC specimens, the ultimate strength of the No. 4 reinforcing bars was tested to be 109.5 ksi, indicating that the bars would be expected to rupture at an applied load of 23.4 kips. With four of the six test specimens exceeding this capacity, only one failed due to bar rupture.

Typical DEMEC measurements of surface strain are shown in Figure 9. The variation of surface strains confirms that in the specimens with No. 4 bars, most of the deformation in the beam occurred at the interfaces and usually the interface openings were not equal. The surface strains measured within the UHPC pocket were very small as compared to the interface strains. The measurements can be easily understood by comparing the tensile strength of the UHPC (typically around 1 ksi) to the bond strength of UHPC/VHPC to precast concrete (typically around 0.3 ksi). Because the bond strength is lower, it can be expected that the interface will crack first in the region of constant moment. Once the interface cracks, the total tension force is carried across the interface by the reinforcing bar. Within the pocket, the tension force is shared by the reinforcing bar and the UHPC up to the limiting strain of the UHPC. It is therefore expected that the strains within the pocket are much smaller than the strains across the interface.

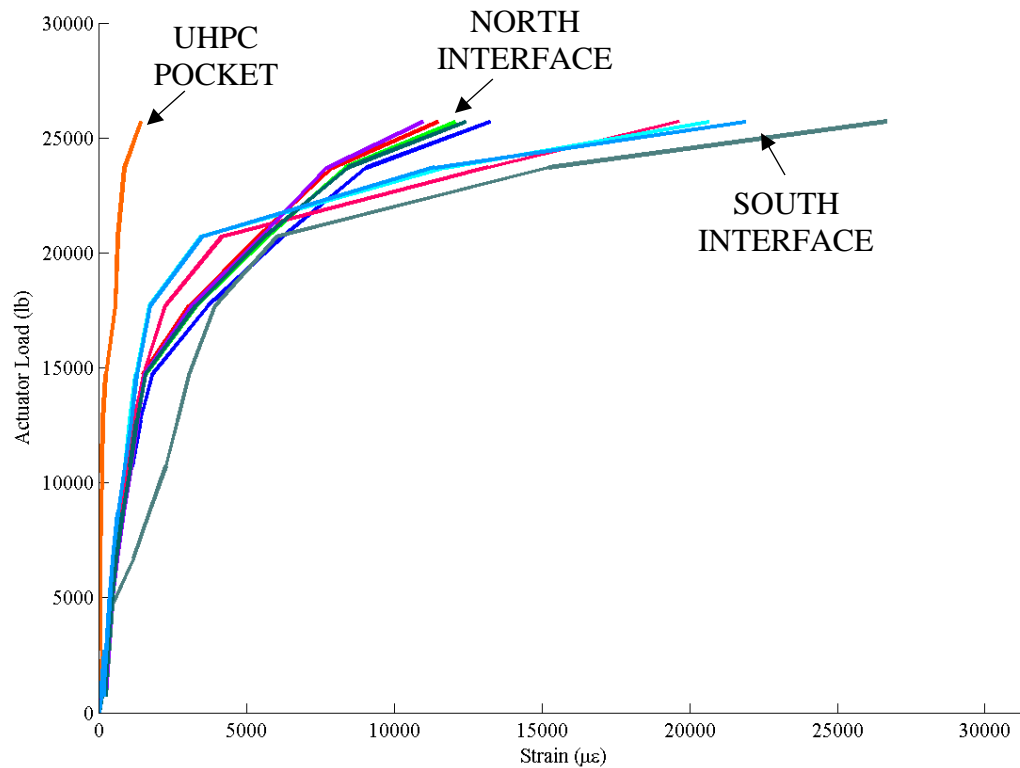


Figure 9. Typical DEMEC strain measurements at the top of the beam for specimens with No.4 bars.

SPLICES WITH NO. 6 BARS AND UHPC SPLICE POCKET FILLER

The splice lengths tested with No. 6 bars ranged from 5 in. to 8 in. As described previously, the tests were performed in two stages, with the first two tests having an equal area of compression and tension reinforcement (two No. 6 bars), and the second two tests having a greater amount of compression reinforcement (two No. 8 bars and one No. 7). The typical details are shown in Figure 2. The nominal strengths of the specimens were calculated based on the yield strength of the tension reinforcement and the moment arm between the compression and tension reinforcement. For this basic calculation, the contribution of the UHPC to flexural strength is ignored.

$$A_s = 0.44 \text{ in}^2 \times 2 = 0.88 \text{ in}^2$$

$$M_n = A_s f_y \times \text{moment arm} = 0.88 \text{ in}^2 \times 60 \text{ ksi} \times 8 \text{ in.} = 422 \text{ in-k}$$

Based on the loading diagram presented in Figure 4, the applied load to result in a 422 in-k moment is:

$$M = \frac{P_{applied}}{2} \times 30in.$$
$$P_{applied} = \frac{M}{15in.} = \frac{422in - k}{15in.} = 28.2 kips$$

The calculated load was compared with the peak loads for all specimens with No. 6 bars. The load vs. deflection behavior displayed by specimens with No. 6 bars is similar to that seen in specimens with No. 4 bars. The specimens with equal areas of steel have a lower deflections and peak loads than those with increased area of steel in compression. The midspan deflections for these specimens did not show a significant increase in magnitude until the interfaces debonded.

The magnitudes of deflections at north and south ends of the specimens for most part of the testing had very small difference in all specimens with No. 6 bars indicating that the actuator load was distributed equally by the spreader beam. The only time when any significant difference occurred was close to failure when the reinforcing bars on one side of the pocket debonded from the UHPC. The load vs. averaged displacement plots for the specimen ends is shown in Figure 10. The midspan deflections did not increase until the specimen had cracked significantly. The midspan deflections, shown in Figure 11, increased rapidly after the interface between the precast element and the UHPC pocket debonded. Similarly, the variation of strains in compressive steel, shown in Figure 12, was linear until the interfaces debonded except for the specimens with equal areas of steel. In these, the non-linear behavior was observed prior to interface debonding simply because the area of steel in compression provided insufficient resistance to the capacity of the beam in tension. The area of steel in compression was increased to prevent yielding. However, yielding and significant non-linear behavior was observed. This occurred due to locating the strain gauges on the bottom of the reinforcing bars causing larger compression than that at the center of the bar, which was considered for the calculation of the nominal capacity.

The load vs. interface displacement plot, shown in Figure 13, indicates the complete debonding of the interface occurred at similar loads which alludes to a level of consistency in the bond strength between different batches of UHPC and a single batch of concrete used to fabricate the precast element. The results of tests on specimens with No. 6 bars are summarized in Table 6.

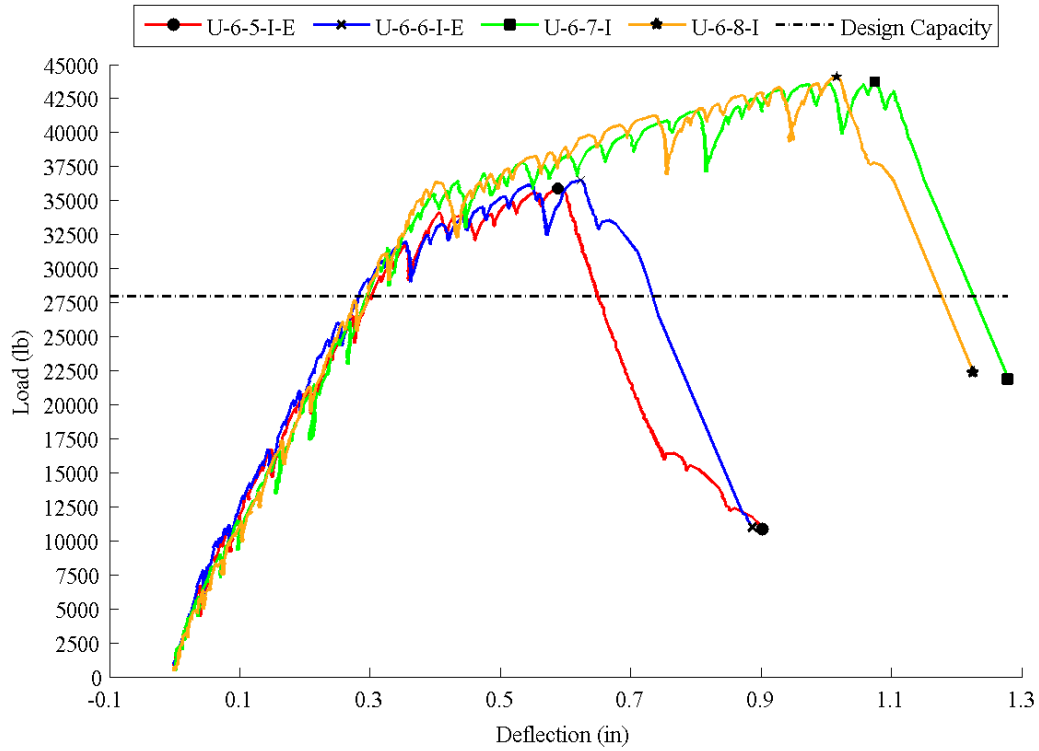


Figure 10. Load vs. average end deflection for all specimens with No. 6 bars.

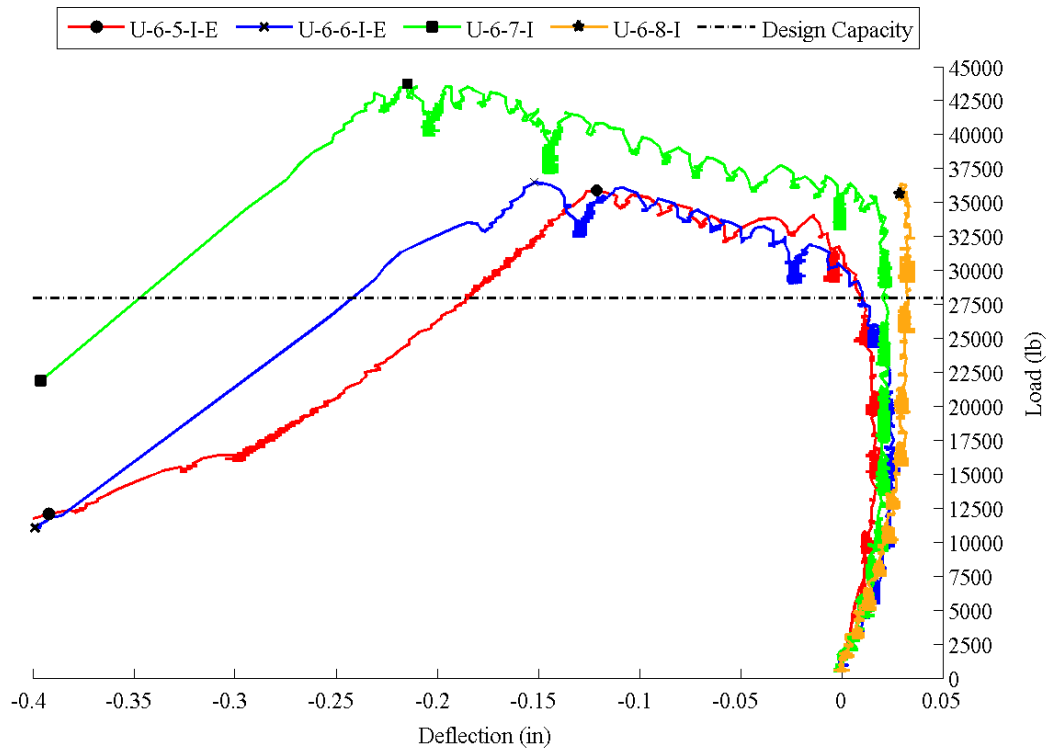


Figure 11. Load vs. midspan deflection for all specimens with No. 6 bars.

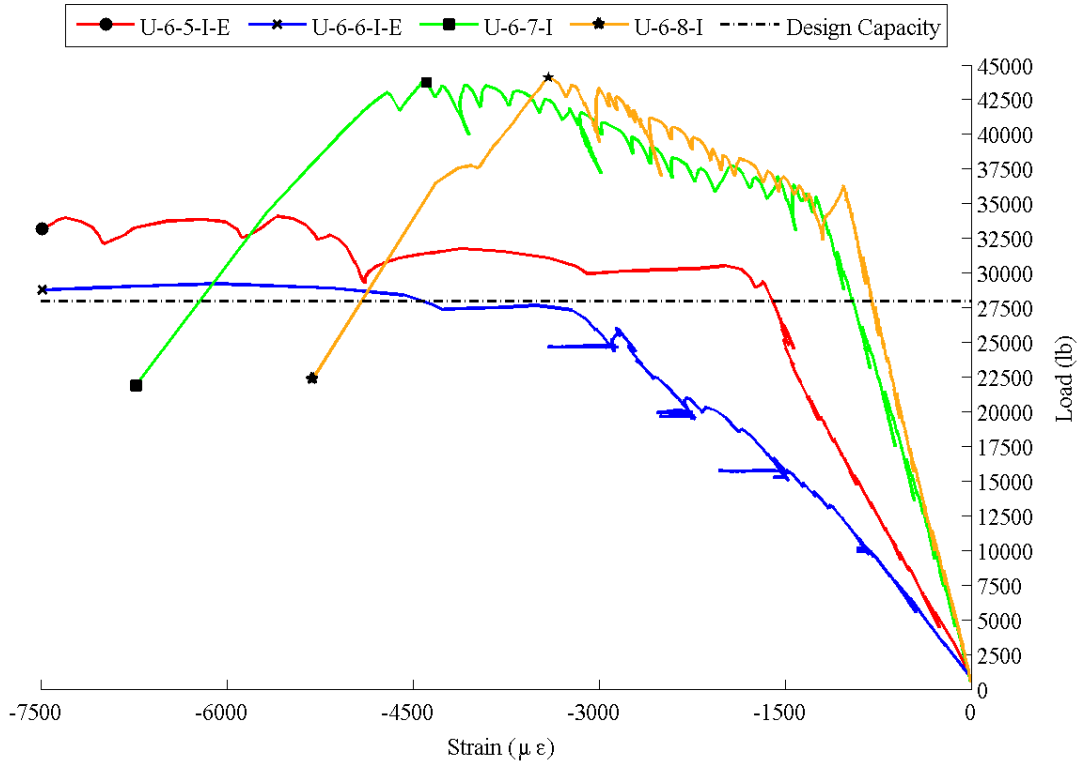


Figure 12. Load vs. average reinforcement strain for all specimens with No. 6 bars.

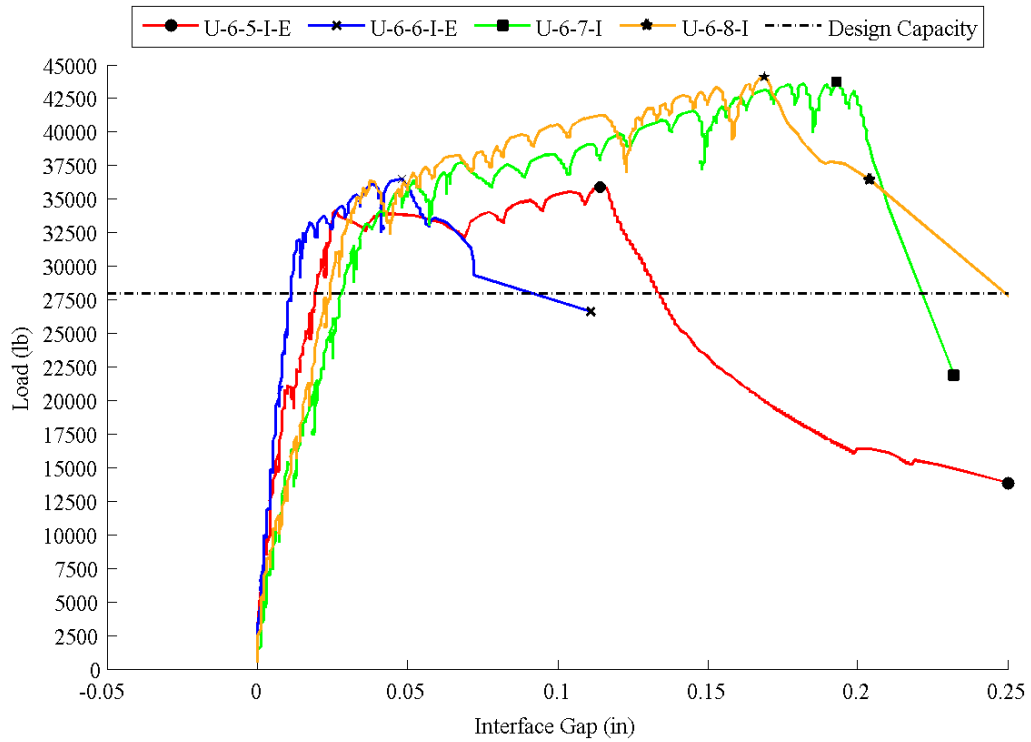


Figure 13. Load vs. maximum interface displacement for all specimens with No. 6 bars.

Table 6. Test Results for Specimens with No. 6 Bars and UHPC

Specimen Designation	Splice Length, in.	Compression Reinforcement	First Cracking Load, lbs	Maximum Load, lbs	Failure Mode
U-6-5-I-E	5	2 No. 6s	7800	35,000	Rebar slip
U-6-6-I-E	6	2 No. 6s	8000	35,700	Rebar slip
U-6-7-I.	7	2 No.8s and 1 No. 7	9000	43,200	Splitting
U-6-8-I.	8	2 No.8s and 1 No. 7	9300	43,500	Splitting

As seen in the test results for specimens with No. 4 bars, comparing the load calculated from nominal capacity to the failure loads presented in Table 6 indicates that all specimens exceeded the yield moment, indicating all tension reinforcement had yielded at the instant of failure. Repeating the same calculations with the ultimate strength of the No. 6 reinforcing bars, of 102 ksi indicates that the bars would be expected to rupture at an applied load of 47.8 kips. None of the four specimens exceeded this capacity, and none failed due to bar rupture. However, other aspects of the specimens' behavior must be investigated to determine an appropriate splice length.

TYPICAL FAILURE MODES OBSERVED

The failures in all specimens, regardless of area of steel in tension, occurred at the interface of the pocket and the precast element. Thirteen specimens out of fourteen failed by bond failure. Only one specimen failed due to tension reinforcement rupture. In all of the specimens, at ultimate, the typically observed cracking pattern is schematically shown in Figure 14. The specimens with UHPC as pocket filler material would show “diagonal cracks” at failure and the VHPC specimens would show “delamination” at failure as shown in Figure 14.

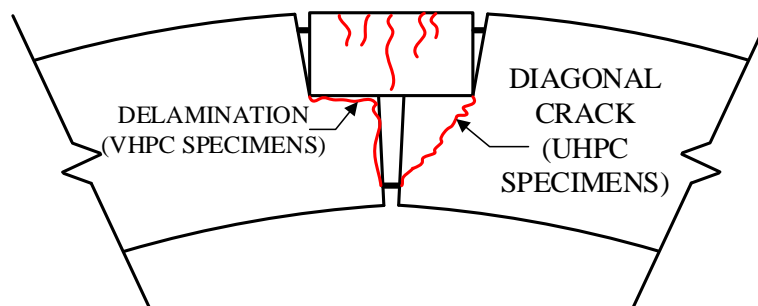


Figure 14. Schematic representation of cracks in the precast element under the splice pocket.

The crack patterns in the pocket were indicative of the type of failure observed in each specimen. The specimens with reinforcing bar slip or pull out displayed large cracks within the pocket. These cracks typically occurred at the end of the reinforcing bar. Such a failure mode is shown in Figure 15.



Figure 15. Large cracks at end of reinforcement due to reinforcing bar pull out.

Specimens with another mode of bond failure would display flexural cracks as well as splitting cracks. These are shown in Figure 16.



Figure 16. Interface separation and splitting cracks seen in pocket.

The specimens with No. 6 bars and equal areas of steel displayed a peculiar form of cracks. Splitting cracks occurred at the level of reinforcement and connected with the interface “cracks” and existing flexural cracks over the section with the foam pad at midspan. This mode of failure was caused by the short length of the splice reinforcement i.e. the stiffness of the reinforcement bars projecting from the precast element and the splice bars was sufficient to precipitate splitting cracks and then separate the pocket into two parts. Essentially the short length of the reinforcement caused a “prying” action on the UHPC pocket. The stiffness of the bars in the UHPC pocket was high enough to prevent the reinforcing bars from deforming with the UHPC in the pocket in a compatible manner.



Figure 17. Side view of UHPC pocket in specimen U-6-6-I-E after failure showing the effect of prying
Finally, the specimen with reinforcing bar rupture is shown in Figure 18.



Figure 18. Ruptured reinforcing bars.

DISCUSSION AND ANALYSIS

The principal answer sought in this testing was whether the length of splices was sufficient to yield the tension reinforcement. The magnitude of strain in tension was not measured directly so the stress in the tension reinforcement must be determined indirectly. Based on the strains measured in the testing it was clear that yielding occurred in compression reinforcing bars. The specimens with a greater amount of compression steel than tension steel were not expected to yield, based on an average stress in the bars. However, the strain gauge was placed on the bottom of the bars, and there was a significant strain gradient through the depth of the bars. Therefore, even if the strain at the center of the bar was less than yield, the strain gauge on the bottom of the bar could indicate yielding. To get a better understanding of the behavior of the cross-section, and thereby determine the forces in the spliced bars, a strain compatibility analysis was performed on the four tested cross-sections. The following section describes the assumptions made in the analysis.

STRAIN COMPATIBILITY ANALYSIS

The beam specimens were analyzed in greater detail by modeling the constitutive properties of steel and the pocket filler material. The cross-section of the beam specimens at which the failure initiated was discretized into slices of equal thickness. The cross-section at which the failure initiated resembled that shown in Figure 2, which consisted of the top reinforcement and pocket material in tension and the bottom steel bars in compression. The equilibrium of the beam cross-section was calculated by integrating the stresses in the slices and equating the forces in compression and tension.

The constitutive relationships of steel and the pocket filler material were determined from material property tests. The steel stress-strain relationship was determined from the average properties of the steel reinforcing bars tested. The average values encompassed the stress strain values of steel reinforcement of all sizes. The constitutive relationship for steel was simplified by linearizing all the curves. The strain hardening behavior of steel was defined by a bilinear relationship. The constitutive relationship for steel is shown in Figure 19 and the equations that define the plot are shown in Table 7.

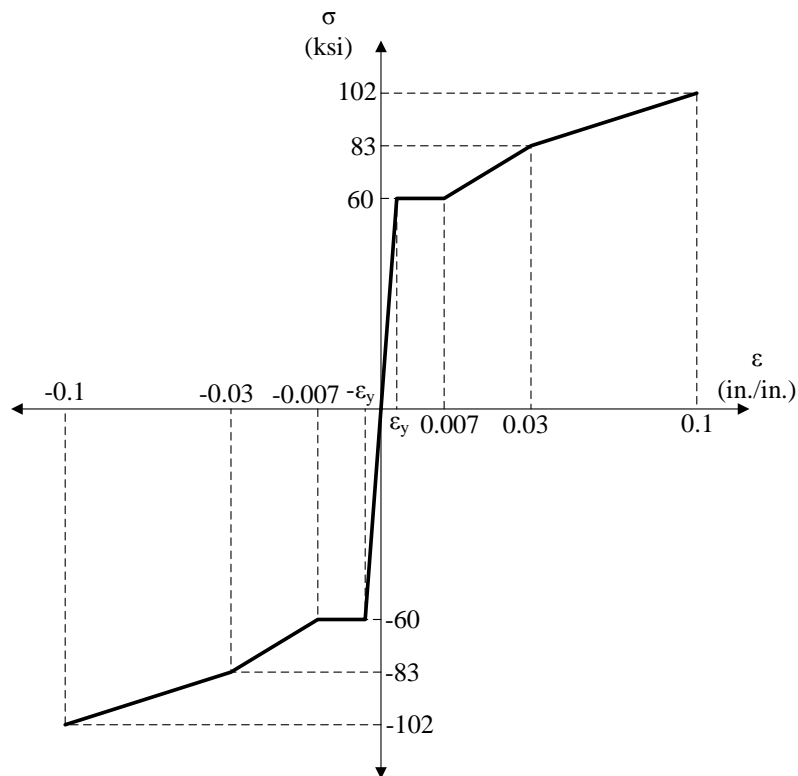


Figure 19. Stress-Strain relationship for reinforcing steel.

Table 7. Equations for steel stress and strain

Strain Range	Equation
$\varepsilon_s > 0.03$	$F_s = 85 + (\varepsilon_s - 0.03)214 \leq 102 \text{ ksi}$
$0.007 \leq \varepsilon_s < 0.03$	$F_s = 60 + (\varepsilon_s - 0.007)1087$
$\varepsilon_y \leq \varepsilon_s < 0.007$	$F_s = 60$
$-\varepsilon_y \leq \varepsilon_s < \varepsilon_y$	$F_s = \varepsilon_s E_s$
$-0.007 < \varepsilon_s \leq -\varepsilon_y$	$F_s = -60$
$-0.03 < \varepsilon_s \leq -0.007$	$F_s = -60 + (\varepsilon_s + 0.007)1087$
$\varepsilon_s < -0.03$	$F_s = -85 + (\varepsilon_s + 0.03)214 \geq -102 \text{ ksi}$

Similarly, the constitutive relationship for the pocket filler material, UHPC and VHPC, was defined on the basis of the model described by Russell and Graybeal (2013). The model defines a bilinear stress-strain behavior in tension. The stress in the pocket filler material varies linearly until the initiation of cracking. The stress in the initial linear elastic portion can be calculated by multiplying the strain value with the elastic modulus of the material determined from the compressive tests. After initiation of cracking the stress remains uniform until a limiting strain. After reaching a limiting point the stress becomes zero. The constitutive model of the pocket filler material is shown in Figure 20.

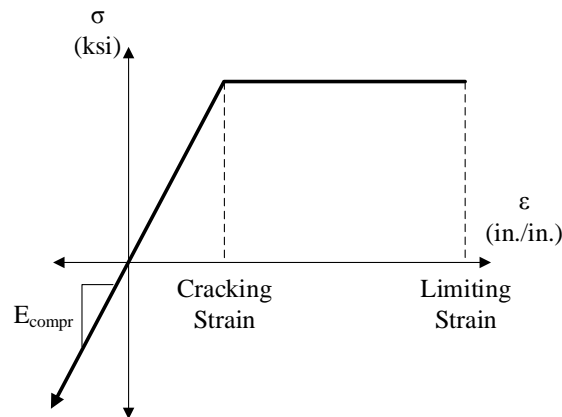


Figure 20. Constitutive model for UHPC and VHPC.

Over the period of testing, a wide variance was observed in the material properties of the pocket filler material. Hence, a simple average of the elastic modulus and compressive and tensile strengths did not represent a typical material behavior as assumed and observed in steel. Therefore, a range of values was adopted from the material property tests on the pocket filler material. This range is shown in Table 8.

Table 8. Parameters for UHPC constitutive model

Parameter	High Value	Low Value
Modulus of Elasticity	8000 psi	6000 psi
Cracking stress	1.0 ksi	0.25 ksi
Limiting Strain	0.010	0.0005

The analysis was performed by assuming either of the high and the low values to observe the comparison of the data between the calculated strains versus the measured strains. Typically, it was observed that the bond strength of the pocket filler material and the concrete in the precast element was lower than the tensile capacity of pocket filler material on the basis that the interface would separate and the tension across that section would then be carried by the steel reinforcing itself. Overall, the assumption of the low values, as shown in Table 8, were representative of the interface bond. The bond strength between the two materials was not explicitly determined for these tests. Even if the actual bond strength was known, there is an inherent difficulty in measuring the modulus of elasticity of the interface of two materials and consequently the stress-strain behavior. The assumption of the low range values, especially the small value for limiting strain, represented the bond strength more than the behavior of the pocket filler material.

The results of the analysis were plotted as load vs. compression reinforcement strain and were compared with the load vs. compression reinforcement strain from test data. The procedure to calculate one point on the load vs. strain-at-the-bottom-of-the-bar curve was as follows:

1. Select the strain at the centroid of the compression bar for the point to be calculated.
2. Select a neutral axis depth, c , measured from the center of the compression bar.
3. Based on strain and c , calculate the curvature, $\phi = \epsilon/c$.
4. Based on the strain and curvature, determine the strain at each layer of steel and in the pocket filler material.
5. Based on strains and constitutive relationships, determine the stresses and forces in the UHPC and steel bars.
6. Sum stresses, and iterate on c , until the forces sum to zero.
7. Based on c , calculate the strain in the center of tension steel. Calculate the stress in tension steel from the constitutive relationship.
8. Based on c , calculate internal moment.
9. Based on internal moment and the statics of beam specimens calculate the externally applied load.

The pocket was discretized into twenty slices of equal depths and widths. Similarly, the reinforcing bars in compression were discretized into twenty slices of equal depths. The width of each slice was independently determined from geometry and the width of the slice at the mid-depth was assumed as the average width. This led to a small error in the calculation of the reinforcing bar area, but the level of discretization prevented the error from exceeding 3% of the gross area of the steel in compression. It is to be noted that the steel reinforcement in tension was not discretized into sliced areas and the magnitude of stress and strain was sought at the mid-depth of the bars. For both the pocket filler material and compression steel, the strain was calculated at the center of each slice and the stress was determined from the constitutive models described earlier. The location of the beam neutral axis was iterated such that the forces in tension and compression balanced.

Once equilibrium was established, the bending moment induced in the section was calculated. These steps were repeated till the tension steel reinforcement would reach a stress

magnitude equivalent to the average rupture stress measured in material property testing of steel. The strain compatibility analysis was performed for all four specimen types. The results of the strain compatibility analysis for beams with No. 4 bars at top and bottom with UHPC are shown in Figure 21, results specimens with No. 4 bars in tension only and UHPC are shown in Figure 22, results for specimens with No. 6 bars with equal areas are shown in Figure 23, results for specimens with No. 6 bars in tension only are shown in Figure 24 and finally the results for specimens with No. 4 bars and VHPC are shown in Figure 25.

As mentioned earlier, the load vs. compression reinforcement strain variation from the test data was compared with the results of the strain compatibility analysis. The applied loads were calculated from the bending moment induced in the section due to equilibrium of internal forces. This internal moment was equated with the bending moment generated by the externally applied loads and thus the loads were calculated.

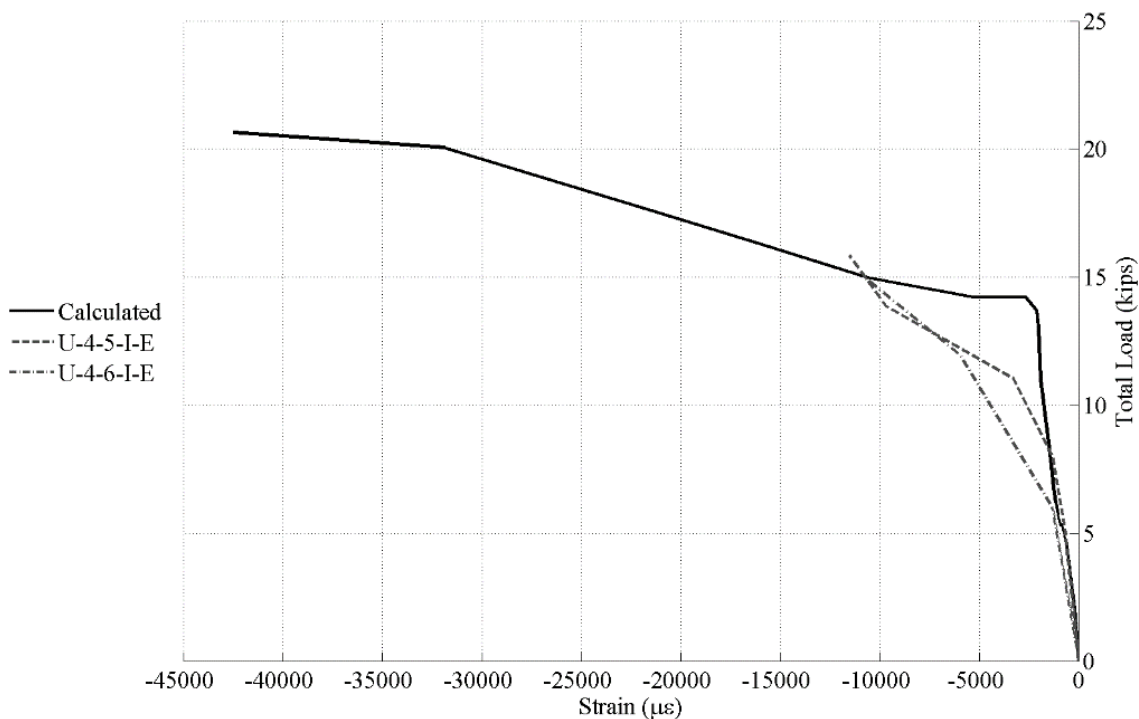


Figure 21. Comparison of strains (measured and calculated) for beams with No. 4 bars top and bottom.

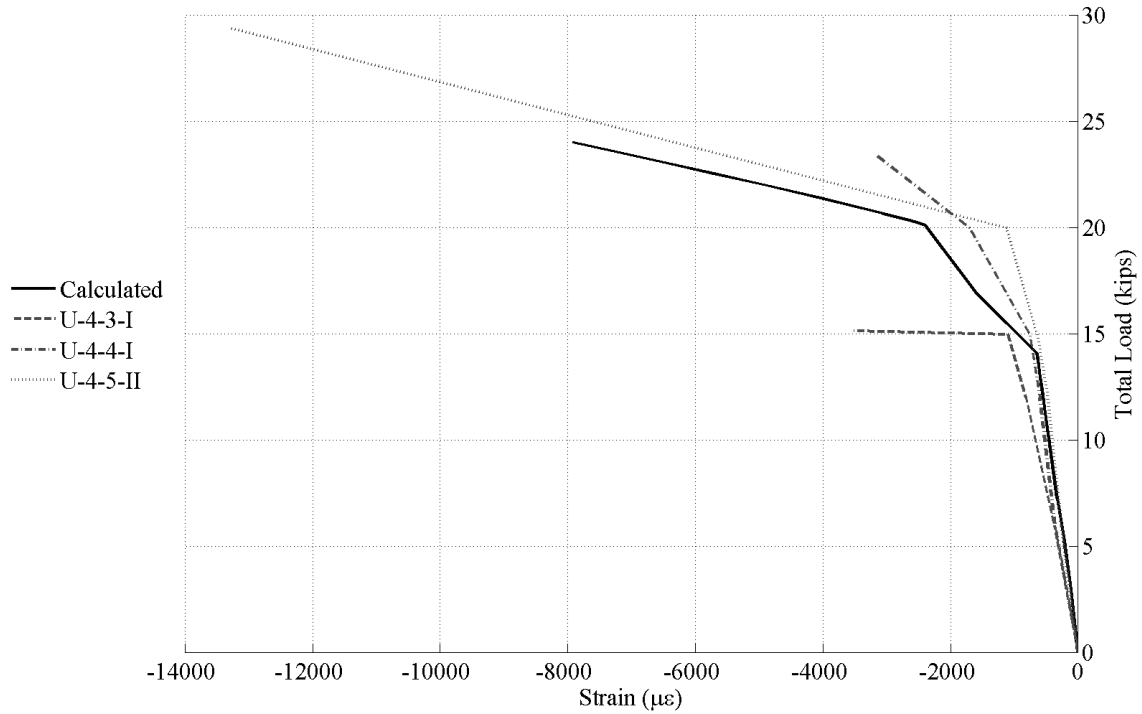


Figure 22. Comparison of strains (measured and calculated) for beams with No. 4 bars at top only.

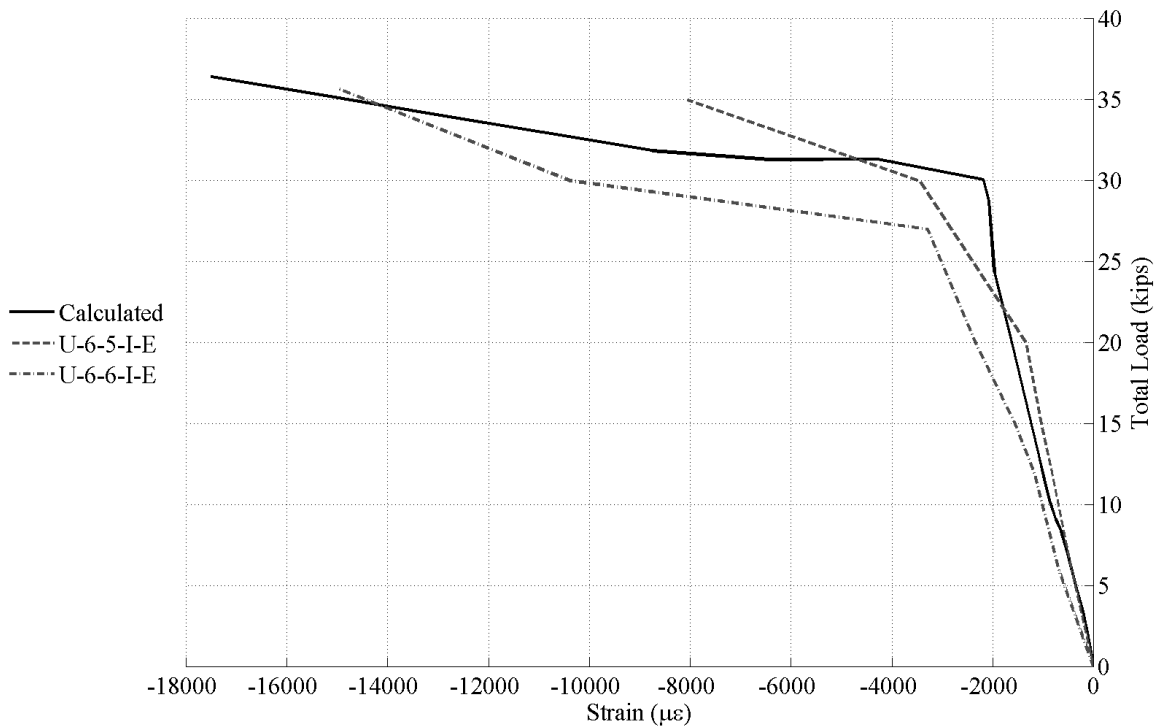


Figure 23. Comparison of strains (measured and calculated) for beams with No. 6 bars top and bottom.

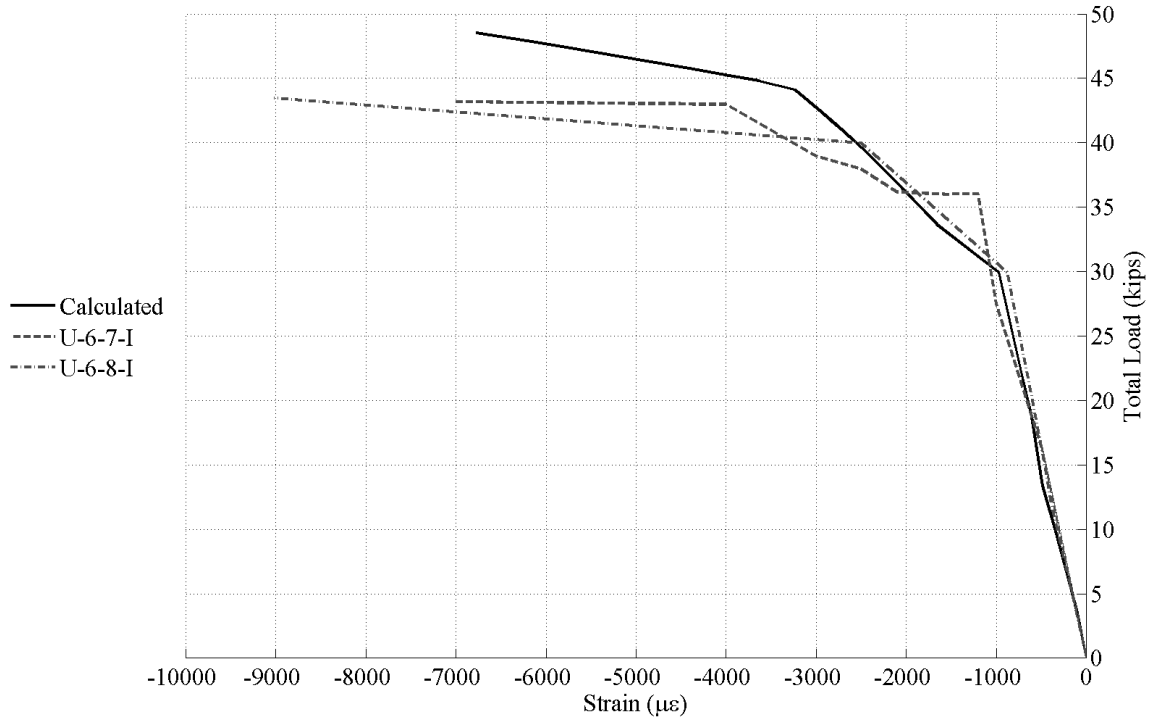


Figure 24. Comparison of strains (measured and calculated) for beams with No. 6 bars top only.

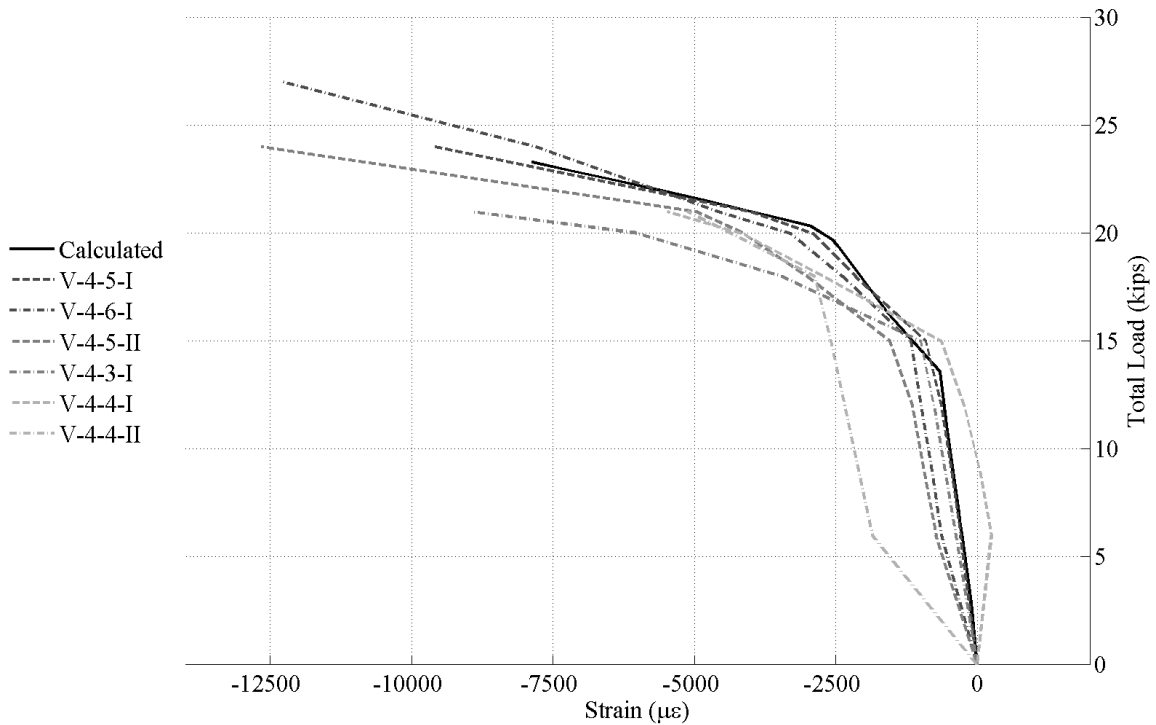


Figure 25. Comparison of strains (measured and calculated) for beams with VHPC as pocket filler.

Overall, a good agreement was observed between the strain compatibility analysis and the measured data. In most instances where a difference in predicted vs. observed behavior was

noted, the deviation was caused by the averaging of steel material properties as well as the inherent variability in the bond strength between the pocket filler material and the concrete in the precast element. For all other specimens, the behavior observed in the complete test could be compared with the predicted behavior except for specimens with No. 4 bars at top and bottom. Typically, the magnitude of strain caused by the application of the peak load was selected. Now, for the specimens that displayed lower strains at ultimate than those predicted by the strain compatibility analysis, the ultimate strain in compression steel measured from tests was selected. Whereas, for the tests in which the measured ultimate strain was higher, the predicted ultimate strain was used.

From the selected strain in compression the corresponding strain in tension was calculated. Finally, the stress in tension steel was then calculated from the constitutive model shown in Figure 19 on the basis of the calculated strains. The scheme of selection of ultimate compressive strains is shown in Figure 26. On the basis of the comparison of the measured data and the analysis the strains and stresses in the tension steel were calculated and are reported in Table 9.

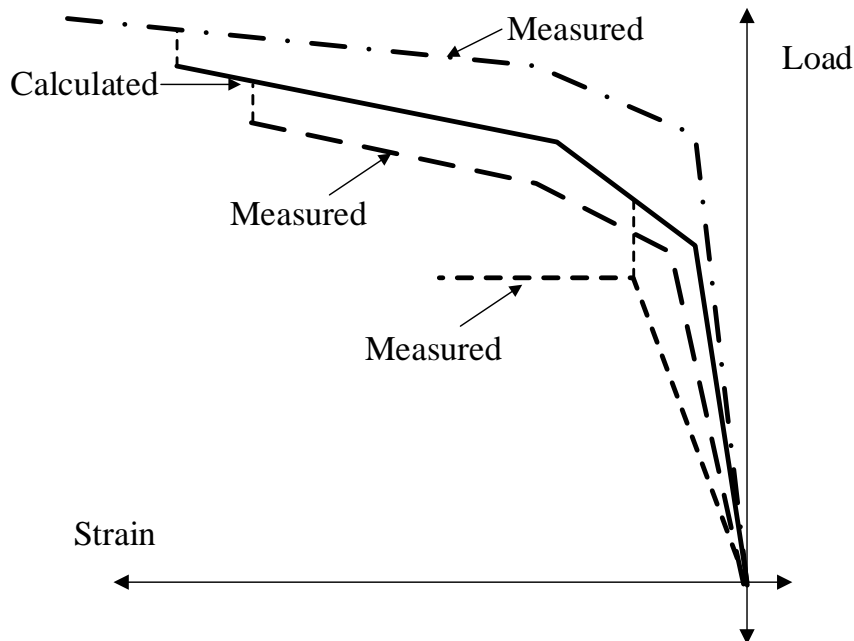


Figure 26. Method for selecting strain in compression bars at ultimate.

Table 9. Maximum strains and stresses in tension reinforcement

Specimen Designation	Splice Length, in.	Selected Strain in Compression, (in. /in.)	Maximum Strain in Tension Steel, (in. /in.)	Maximum Tension Stress, ksi
U-4-5-I-E	5	0.0115	0.01	63.3
U-4-6-I-E	6	0.0107	0.009	62.2
U-4-3-I	3	0.0011	0.016	69.8
U-4-4-I	4	0.00315	0.04	87.1
U-4-5-II	5	0.0079	0.1	100
V-4-5-I	5	0.008	0.092	98.3
V-4-6-I	6	0.008	0.092	98.3
V-4-5-II	5	0.008	0.092	98.3
V-4-3-I	3	0.008	0.092	98.3
V-4-4-I	4	0.005	0.092	92.8
V-4-4-II	4	0.005	0.092	92.8
U-6-5-I-E	5	0.008	0.0078	60.9
U-6-6-I-E	6	0.015	0.013	66.5
U-6-7-I	7	0.0068	0.067	92.9
U-6-8-I	8	0.0068	0.067	92.9

As observed in Table 9, the tension reinforcement in all specimens attained the yield stress. Therefore, based solely on the criteria of yield stress, a 3 in. splice length for a No. 4 bar and a 5 in. splice length for a No. 6 bar are adequate in UHPC. However, ductility should also be considered. ACI 318-11 requires that for a beam to be considered tension controlled, the tension reinforcement must reach a strain of at least 0.005, which was exceeded by all the specimens. Based on this analysis, it is somewhat more conservative to recommend a 5 in. splice for No. 4 bars and a 6 in. splice for No. 6 bars in UHPC. Although it is possible to use shorter splice lengths with No. 4 bars, there is a concern that with such short splice lengths any unintended reduction in length during fabrication would reduce the splice and hence the strength and ductility of the splice below the expected value. Hence, to ensure at least a 4 in. splice is provided the researchers recommend the use of a 5 in. splice with No. 4 bars. Similarly, for No. 6 bars a 6 in. splice is recommended.

CONCLUSIONS

The testing program was performed to ascertain the performance of UHPC and VHPC as filler materials to facilitate the use of short splice lengths in longitudinal joints between adjacent precast member bridges. Based on the results of the static tests performed on simply supported beam specimens the following conclusions were made,

1. Splice lengths with No. 4 bars of 4 in. and longer were sufficient to yield the tension reinforcement prior to failure.
2. Splice length of No. 4 bars of 5 in. is recommended to ensure ductility.
3. Splice lengths with No. 6 bars of 5 in. and longer were sufficient to yield the tension reinforcement prior to failure.
4. Splice length of No. 6 bars of 6 in. is recommended to ensure ductility.
5. The additional 1 in. length was recommended to account for construction tolerances. The additional length is essentially akin to providing a resistance factor against fabrication errors and poor UHPC/VHPC quality.
6. UHPC and VHPC provided a comparable performance in terms of the minimum length of splice required per material for No. 4 bars.
7. In terms of material costs, VHPC was a cheaper material than UHPC. VHPC contains a higher percentage of aggregates than UHPC per cubic foot of concrete mix.
8. Both mixes were easy to mix, handle and place. The use of UHPC as a connection material for field cast joints in precast elements is becoming quite prevalent. VHPC use is not as prevalent as UHPC.
9. Although UHPC was more expensive than VHPC, the durability of UHPC has been tested and certified. More study is needed for VHPC in terms of durability.
10. Finally, joints need to be sealed well as both materials are self-consolidating and can leak.

REFERENCES

- Graybeal, B. A. "Material Property Characterization of Ultra-High Performance Concrete," 2006, 190p.
- Morcous, G., M. Maguire and M. K. Tadros "Welded-wire reinforcement versus random steel fibers in precast, prestressed concrete bridge girders," *PCI Journal*, V. 56, No. 2, Spring 2011, pp. 113-120.
- Russell, H. G. "Adjacent Precast Concrete Box Beam Bridges: Connection Details. A Synthesis of Highway Practice," 2009, 86p.
- Russell, H. G. and B. A. Graybeal "Ultra-High Performance Concrete: A State-of-the-Art Report for the Bridge Community," 2013, 176p.

ACKNOWLEDGEMENTS

The researchers would like to thank the Center for Advanced Infrastructure and Transportation at Rutgers University and the Virginia Center for Transportation Innovation and Research for funding this research. The contributions of Elkem, Titan America, and Bekaert are also graciously acknowledged. Finally, the researchers would also like to thank Dennis Huffmann, Brett Farmer and Dr. David Mokarem for their support in the laboratory.